865

Experimental investigation of picosecond pulse reflection from fiber gratings

D. Taverner, D. J. Richardson, J.-L. Archambault, L. Reekie, P. St. J. Russell, and D. N. Payne

Optoelectronics Research Centre, University of Southampton, Hants SO9 5NH, UK

Received June 27, 1994

The dispersion of picosecond pulses on reflection from efficient photorefractive fiber gratings is explored experimentally. Unlike simple measurements of reflectivity, this approach allows both the amplitude and the phase of the grating response to be probed as a function of frequency.

The development of techniques for writing high-reflectivity fiber Bragg gratings[1-3] has created a wide range of new possibilities for fiber-based devices. These offer advantages of simplicity, compactness, robustness, and cost over bulk-optic equivalents. A number of applications rely solely on the spectral filtering properties of the grating structure, requiring no knowledge of the phase response of the grating, e.g., the use of a fiber grating as a bandwidth-limiting element in a single-frequency fiber laser.[4] However, in many applications, particularly those involving ultrashort pulses, e.g., pulse compression,[5] the grating dispersion characteristics can be of considerable, if not prime, importance and require a detailed understanding. This dispersion arises from both the spectral shaping that is due to the nonlinear form of the spectral intensity response and the frequency-dependent phase response. In this Letter we report the results of an experimental investigation of the effects of grating dispersion on the reflection and transmission of transform-limited picosecond optical pulses from uniform fiber gratings.

The experimental configuration is shown in Fig. 1. Picosecond, transform-limited, hyperbolic-secant pulses were obtained from an all-fiber, polarization-maintaining (P.M.) figure-eight fiber soliton laser.[6] The pulses were passed through an isolator and launched by a 3-dB coupler into the fiber grating under test. The grating itself was mounted in a jig that permitted strain tuning of the reflection peak wavelength of the grating and, hence, the wavelength offset from the central wavelength of the incident pulses ($\approx$1.532 μm). The maximum grating wavelength shift used was $\sim$5 nm toward longer wavelengths from the unstrained reflection peak wavelength. We investigated the pulse response of the grating in the temporal and spectral domains by measuring the autocorrelation function (ACF) and the optical spectrum of the reflected or transmitted pulses. The source permitted tuning of the pulse duration (and corresponding optical bandwidth) over the range 2.3–6 ps with no significant degradation in quality. These two degrees of flexibility enabled us to examine the grating response over a wide range of system parameters. Finally, a pair of polarization controllers (P.C.'s) was included to permit investigation of the effects of the input polarization state on the grating response.

In modeling the grating response we employed conventional coupled-mode theory.[7] By assuming that only a single reflected and transmitted mode are significantly coupled by the grating, we can obtain the following pair of equations:

$$\frac{dA_2(z, \Delta\beta)}{dz} = j\kappa^*(z)A_1(z, \Delta\beta)\exp(-j\Delta\beta z),$$

$$\frac{dA_1(z, \Delta\beta)}{dz} = -j\kappa(z)A_2(z, \Delta\beta)\exp(j\Delta\beta z), \quad (1)$$

where $A_1(z, \Delta\beta)$ is the complex electric-field amplitude of the forward-propagating mode and $A_2(z, \Delta\beta)$ is that of the backward-propagating mode, both being functions of distance (z) and the wave-vector offset from that at the grating Bragg wavelength ($\Delta\beta$). $\kappa(z)$ is the grating coupling coefficient that is in general dependent on the length, modulation depth, and form of the grating; for the case of a uniform sinusoidal index modulation it is a constant, given by $\kappa = \pi\Delta n/\lambda_{\text{Bragg}}$, where Δn is the zero-to-peak amplitude of the modulation. In this case we can obtain exact solutions for the reflection and transmission amplitudes:

$$r(\Delta\beta) = A_2(0, \Delta\beta) = \frac{-j\kappa^* \sinh(SL)}{S\cosh(SL) + j\frac{\Delta\beta}{2}\sinh(SL)},$$

$$t(\Delta\beta) = A_1(L, \Delta\beta) = \frac{jS\exp\left(j\frac{\Delta\beta}{2}L\right)}{S\cosh(SL) + j\frac{\Delta\beta}{2}\sinh(SL)}, \quad (2)$$

where L is the length of the grating and $S^2 = \kappa^*\kappa - (\Delta\beta/2)^2$.

We calculated the reflected and transmitted pulse field amplitudes by multiplying the grating frequency response by the relevant soliton field frequency spectrum. To compare our calculations with the experimental measurands, we compute the corresponding

0146-9592/95/030282-03$6.00/0

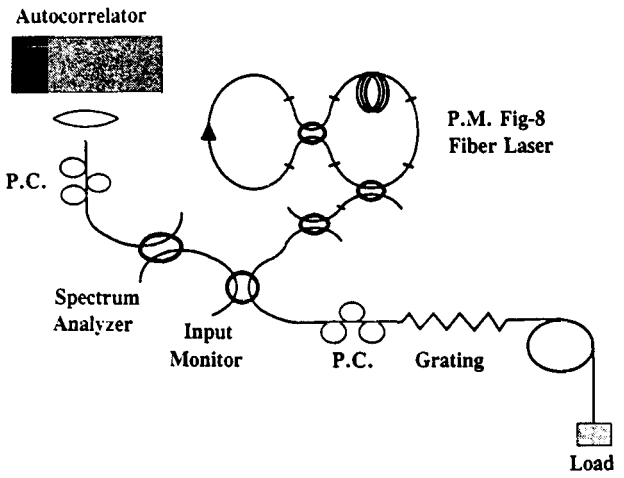

Fig. 1. Experimental configuration.

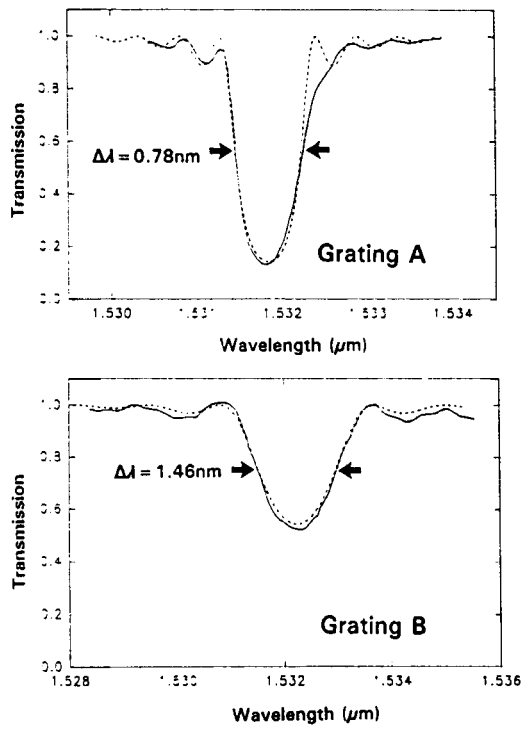

Fig. 2. Experimental (solid curves) and fitted (dashed curves) transmission characteristics of gratings A and B.

spectral intensity half-width and, by Fourier transform into the temporal domain, the ACF half-width. In all the experiments that follow the broadening factors that we define are specified in terms of the broadening of the ACF and spectral half-widths; no further account is taken of the detailed temporal pulse shaping.

Two Type I gratings were examined, both fabricated with a multipulse-exposure, UV interferometric side-writing technique.[1] Grating A had a peak reflectivity $R = 0.86$ at 1.532 μm, with spectral half-width $\Delta\lambda_g = 0.78$ nm, and grating B had $R = 0.47$ at 1.531 μm and $\Delta\lambda_g = 1.46$ nm. The spectral transmission characteristics of the unstrained gratings are presented in Fig. 2, along with the best-fit grating response function used to model the reflection and transmission data. From these fits we estimate grating A to have a length of 1.6 mm and a peak refractive modulation depth of 0.68×10^{-3}; similarly, grating B was 0.6 mm long with a peak modulation depth of 0.92×10^{-3}. The estimated grating lengths are consistent with the lengths of fiber exposed during the grating writing process.

Initially the reflection and transmission of the gratings were investigated as a function of wavelength separation, $\Delta\lambda_{offset}$, between the peak of the grating response and the peak of the pulse spectrum. Figure 3 shows plots of the observed pulse half-width broadening factors versus $\Delta\lambda_{offset}$ for the reflection of 5.6-ps hyperbolic-secant pulses from grating A ($\Delta\lambda_{pulse}/\Delta\lambda_g = 0.56$, where $\Delta\lambda_{pulse}$ is the pulse spectral half-width) and 2.9-ps hyperbolic-secant pulses from grating B ($\Delta\lambda_{pulse}/\Delta\lambda_g = 0.59$) in both the temporal and spectral domains. Minimum temporal broadening factors of 35% and 50% at wavelength offset $\Delta\lambda_{offset} = 0$ for gratings B and A, respectively, are observed. Increased broadening and pulse deformation are observed as the reflection peak moves from the pulse center until $\Delta\lambda_{offset}/\Delta\lambda_g \approx 1$, where the pulse is observed to become multipeaked. Superimposed upon the plots in Fig. 3 are the theoretical pulse-broadening factors obtained by fitting the grating response functions in Fig. 2 to the solutions of coupled-mode theory for a uniform sinusoidal grating. The theory is found to be in good agreement with the experimentally observed results. In addition, the detailed shapes of the calculated spectra and ACF's are in good agreement with those measured experimentally. In Fig. 4 we present data for the transmission of 3.1-ps hyperbolic-secant pulses through grating B ($\Delta\lambda_{pulse}/\Delta\lambda_g = 0.54$). Well away from the reflection peak, minimum broadening is observed; however, within the transmission band significant pulse distortion is obtained, and once again the experimental results are found to agree well with those theoretically predicted. We observed no significant polarization-dependent response from these particular gratings on either reflection or transmission. Strong polarization sensitivity, with large deviation from the expected reflection characteristics,

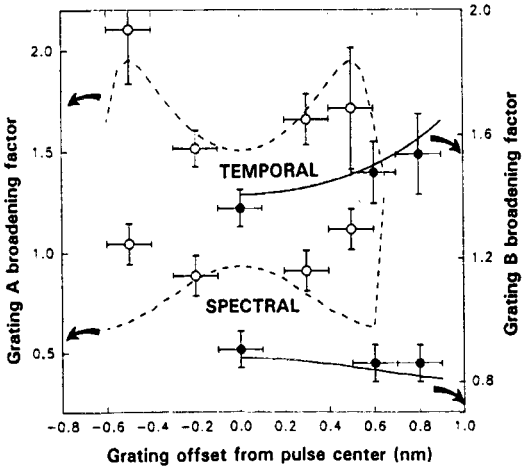

Fig. 3. Experimental (points) and theoretical (curves) autocorrelation half-width and spectral half-width broadening factors for 5.6-ps hyperbolic-secant pulse reflection from grating A and 2.9-ps hyperbolic-secant pulse reflection from grating B.

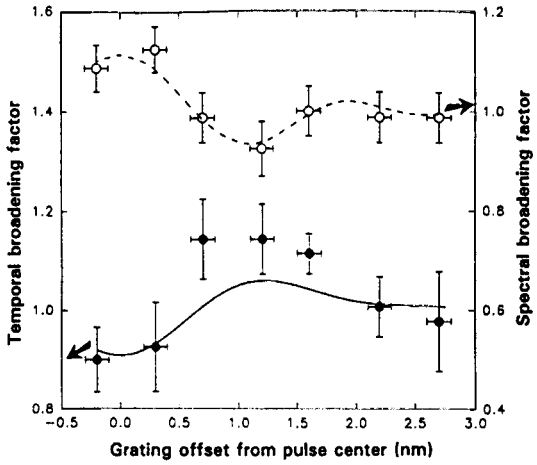

Fig. 4. Experimental (points) and theoretical (curves) autocorrelation half-width and spectral half-width broadening factors for transmission of a 3.1-ps hyperbolic pulse through grating B.

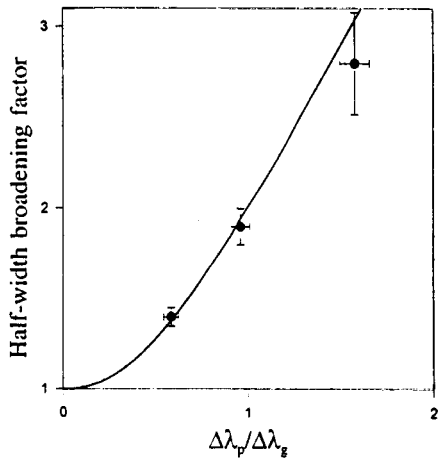

Fig. 5. Experimental (points) and theoretical (curve) pulse broadening on reflection at $\Delta\lambda_{offset} = 0$ for various $\Delta\lambda_p/\Delta\lambda_g$. Theoretical curve is based on the 86% reflectivity, 0.78-nm-bandwidth grating (grating A).

was observed when longer, high-reflectivity (12-mm) gratings were examined. This particular grating gave rise to two distinct reflection peaks in the temporal domain, separated by ≈70 ps, which were reducible to one by rotation of the polarization state. These peaks are believed to result from an intensity dip in the middle of the writing beam, which was known to suffer from poor spatial coherence and beam quality. The origin of the polarization sensitivity is not yet fully understood.

By varying the duration of the pulses incident on the gratings, thus varying the spectral width of the optical pulses and consequently $\Delta\lambda_{pulse}/\Delta\lambda_g$, we obtained a plot of broadening factor as a function of $\Delta\lambda_{pulse}/\Delta\lambda_g$. We were able to vary $0.2 < \Delta\lambda_{pulse}/\Delta\lambda_g < 1.5$ with the soliton spectrum centered on the grating in all instances, i.e., $\Delta\lambda_{offset} = 0$. The results are presented in Fig. 5 along with a theoretical curve based on the coupled-mode theory fit to the 0.78-nm-bandwidth, 86% reflectivity grating (grating A). It can be seen that for $\Delta\lambda_{pulse}/\Delta\lambda_g > 0.2$ uniform sinusoidal gratings give significant dispersive and pulse-shaping effects. These effects increase strongly as $\Delta\lambda_{pulse}/\Delta\lambda_g$ increases. Simple pulse propagation calculations show that only a small fraction of the pulse deformation is due to linear dispersion within the grating and therefore could be compensated by simple linear chirp compensation, e.g., linear pulse propagation in a dispersive fiber. However, the theoretical curves presented in Fig. 4 show that for $\Delta\lambda_{pulse}/\Delta\lambda_g < 0.2$ the pulse-shaping effects can be kept small. In this regime the phase response of the grating is almost linear across the bandwidth of the pulse, and in the case of $\Delta\lambda_{offset} = 0$ the grating reflection intensity response is also almost flat.

In conclusion, the results demonstrate that the use of simple uniform fiber gratings for short-pulse applications is likely to be restricted to cases in which the spectrum of the incident light is narrow relative to the grating bandwidth. When this condition is violated significant pulse degradation can occur. The correlation between the experimental results and the coupled-mode theory confirms that the Type I grating manufacturing technique used produces gratings close to the uniform sinusoidal index modulation expected. Although our measurements have been made on very basic structures, the results give us confidence to extend the coupled-mode theory to more complicated gratings, e.g., multigrating arrays and chirped gratings. These more elaborate structures have great potential for applications such as pulse compression and broadband dispersion compensation in transmission systems.[5]

References

1. G. Meltz, W. W. Morey, and W. H. Glenn, Opt. Lett. **14,** 823 (1989).
2. J.-L. Archambault, L. Reekie, P. St. J. Russell, and D. N. Payne, Electron. Lett. **29,** 28 (1993).
3. K. O. Hill, B. Malo, F. Bilodeau, D. C. Johnson, and J. Albert, Appl. Phys. Lett. **62,** 1035 (1993).
4. J. T. Kringlebotn, P. R. Morkel, L. Reekie, J.-L. Archambault, and D. N. Payne, IEEE Photon. Technol. Lett. **5,** 1162 (1993).
5. P. St. J. Russell, J. Mod. Opt. **38,** 1599 (1991).
6. D. Taverner, D. J. Richardson, and D. N. Payne, in *Nonlinear Guided-Wave Phenomena*, Vol. 15 of 1993 OSA Technical Digest Series (Optical Society of America, Washington, D.C., 1993), p. 367.
7. A. Yariv and P. Yeh *Optical Waves in Crystals* (Wiley, New York, 1984), Chap. 6.
8. F. Ouellette, Opt. Lett. **16,** 303 (1991).